Accepted Manuscript

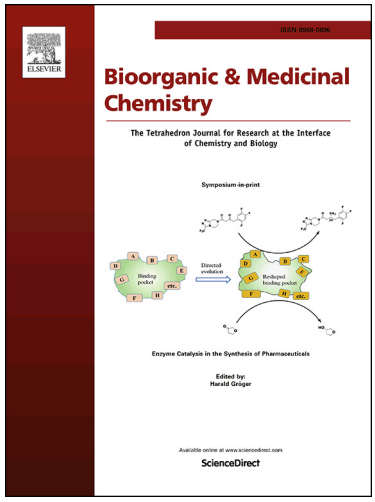

Substituent effect of *N*-benzylated gramine derivatives that prevent the PP2A inhibition and dissipate the neuronal Ca^{2+} overload, as a multitarget strategy for the treatment of Alzheimer's disease

Dorleta Gonzalez, Raquel L. Arribas, Lucia Viejo, Rocio Lajarin-Cuesta, Cristóbal de los Ríos

PII: S0968-0896(18)30196-2
DOI: https://doi.org/10.1016/j.bmc.2018.04.019
Reference: BMC 14302

To appear in: *Bioorganic & Medicinal Chemistry*

Received Date: 29 January 2018
Revised Date: 6 April 2018
Accepted Date: 7 April 2018

Please cite this article as: Gonzalez, D., Arribas, R.L., Viejo, L., Lajarin-Cuesta, R., de los Ríos, C., Substituent effect of *N*-benzylated gramine derivatives that prevent the PP2A inhibition and dissipate the neuronal Ca^{2+} overload, as a multitarget strategy for the treatment of Alzheimer's disease, *Bioorganic & Medicinal Chemistry* (2018), doi: https://doi.org/10.1016/j.bmc.2018.04.019

This is a PDF file of an unedited manuscript that has been accepted for publication. As a service to our customers we are providing this early version of the manuscript. The manuscript will undergo copyediting, typesetting, and review of the resulting proof before it is published in its final form. Please note that during the production process errors may be discovered which could affect the content, and all legal disclaimers that apply to the journal pertain.

ACCEPTED MANUSCRIPT

Substituent effect of *N*-benzylated gramine derivatives that prevent the PP2A inhibition and dissipate the neuronal Ca^{2+} overload, as a multitarget strategy for the treatment of Alzheimer's disease

Dorleta Gonzalez[a], Raquel L. Arribas[a], Lucia Viejo[a,b], Rocio Lajarin-Cuesta[a], Cristóbal de los Ríos[a,b,*]

[a]Instituto Teófilo Hernando and Departmento de Farmacología y Terapéutica, Universidad Autónoma de Madrid, C/ Arzobispo Morcillo, 4, 28029, Madrid, Spain; [b]Instituto de Investigación Sanitaria, Servicio de Farmacología Clínica, Hospital Universitario de la Princesa, 28006 Madrid, Spain

Corresponding author: Cristóbal de los Ríos, e-mail address: cristobal.delosrios@inv.uam.es

Abbreviations: ACh, acetylcholine; AD, Alzheimer's disease; Aβ, amyloid β peptide; $[Ca^{2+}]_c$, cytosolic Ca^{2+}; CALHM1, Ca^{2+} homeostasis modulator-1 channel; FBS, fetal bovine serum; Mem, memantine; NCLX, mitochondrial Na^+/Ca^{2+} exchanger; NFT, neurofibrillary tangles; NMDA, *N*-methyl-D-aspartate; OA, okadaic acid; PAD, PP2A-activating drug; PP2A, phosphoprotein phosphatase 2A; PP2Ac, PP2A catalytic subunit C; *p*NPP, *para*-nitrophenol phosphate; PPP, Ser/Thr phosphoprotein phosphatases; VGCC, voltage-gated Ca^{2+} channels.

ACCEPTED MANUSCRIPT

Abstract

Following the premises of the multitarget-directed ligands approach for the drug R&D against neurodegenerative diseases, where Alzheimer's disease (AD) outstands, we have synthesized and evaluated analogues of the gramine derivative ITH12657 (1-benzyl-5-methyl-3-(piperidin-1-ylmethyl-1*H*-indole, **2**), which had shown important neuroprotective properties, such as blocking effect of voltage-gated Ca^{2+} channels (VGCC), and prevention of phosphoprotein phosphatase 2A (PP2A) inhibition. The new analogues present different substitutions at the pending phenyl ring, what slightly modified their pharmacological characteristics. The VGCC blockade was enhanced in derivatives possessing nitro groups, while the pro-PP2A feature was ameliorated by the presence of fluorine. Chlorine atoms supplied good activities over the two biological targets aimed; nevertheless that substitution provoked loss of viability at 100-fold higher concentrations (10 μM), what discards them for a deeper pharmacological study. Overall, the *para*-fluorine derivative of ITH12657 was the most promising candidate for further preclinical assays.

Keywords: gramine analogues, multitarget strategy, neuroprotection, Ca^{2+} overload, Tau hyperphosphorylation, phosphoprotein phosphatase 2A, Alzheimer's disease

ACCEPTED MANUSCRIPT

1. Introduction

The improvement of life span in developed countries leads to the aging of population and the prevalence of associated pathologies, such as neurodegenerative diseases, where Alzheimer's disease (AD) highlights. AD has a remarkable impact on economy and society, enhanced by the lack of efficient medicines.[1] Hence, the search of both innovative and alternative therapeutic strategies keeps being a priority objective.

Brains of AD patients are mainly characterized by two morphological hallmarks, which are thought to contribute to the neuronal damage in the brain: the senile plaques formed by aggregates of the amyloid β peptide (Aβ),[2] and neurofibrillary tangles (NFT),[3] whose generation has its origin in the altered phosphorylation of the microtubule-stabilizing protein Tau. Every year, a plethora of scientific contributions report possible causes for the rise of these aberrant structures in brain, as well as the pathological consequences that trigger. In the end, therapeutic targets studied for AD are not conveniently validated, what leads to a scientific "tower of Babel" that hinders rational drug discovery programs. Among all of the pharmacological approaches discussed, three of them have prevailed since the 90s, 1) the recovery of the cholinergic transmission, generally by inhibiting the acetylcholine (ACh)-metabolizing enzymes, i.e. the cholinesterases,[4] 2) the removal of the Aβ-formed senile plaques, mainly through the inhibition of enzymes that catalyze the synthesis of Aβ monomers, β-secretase and γ-secretase,[5] and, in a lesser extension, 3) the disruption of the NFT formation in neurons, principally by inhibiting Tau kinases, such as GSK-3β, cdk-5 or PKA.[3] Despite all the scientific efforts spent up to date, none of these strategies have afforded promising crops,[6] as the current marketed drugs [three anticholinesterasics and a *N*-methyl-D-

ACCEPTED MANUSCRIPT

aspartate sensitive (NMDA) receptor blocker][7] only attack the symptoms with limited efficacy.

Given the multifactorial nature of AD, it is widely accepted the hypothesis stating that several physiopathological mechanisms exacerbating neuronal impairment converge to result in an unstoppable neurodegeneration scenario.[8] For this reason, a great part of the scientific community devoted to drug discovery for neurodegenerative diseases has realized that a potential optimal drug should interact with two or more biological targets implicated in AD. Thus, the development of multitarget-directed ligands has given rise to interesting compounds probed for AD.[9-10] Nonetheless, these have commonly focused on the same biological targets, being mostly cholinesterase inhibitors that feature an additional pharmacological property. In this sense, other alternative strategies keep waiting for an opportunity to demonstrate their therapeutic relevance for AD.

Taking into account all the previous evidences, our research group quests innovative approaches to face neurodegenerative diseases that, despite having been proven to be involved in the AD progression, have not been conveniently aimed with the goal of designing new efficient drugs. For instance, we reported the first selective blocker of the recently discovered Ca^{2+} homeostasis modulator-1 channel (CALHM1);[11] the polymorphism P86L of this channel has been implicated in the AD onset, or a new generation of mitochondrial Na^{+}/Ca^{2+} exchanger (NCLX) blockers,[12] on the basis that NCLX plays a chief role in the neurodegeneration triggered by neuronal Ca^{2+} overload. Moreover, we have recently reported the interesting outcomes of some gramine (**1**) derivatives (Fig. 1) that exerted a multitarget profile over voltage-gated Ca^{2+} channels (VGCC) and Ser/Thr phosphoprotein phosphatases (PPP).[13]

ACCEPTED MANUSCRIPT

The neuronal Ca^{2+} overload, highly contributed by altered VGCC opening,[14] is a common event in many neurodegenerative diseases,[15] so several Ca^{2+} antagonists have been positioned as investigational drugs. As far as the Ser/Thr phosphatases, they comply an essential function as dephosphorylating enzymes of the Tau protein, thus counteracting the NFT synthesis, being phosphatase 2A (PP2A) the principal enzyme.[16] Indeed, PP2A is found inactivated or inhibited in both in vivo and in vitro models of AD,[17-18] as well as in post-mortem AD patient brains.[19] Hence, there is currently an increasing interest in developing drugs able to reduce the endogenous inhibition of PP2A, thus named PP2A-activating drugs (PADs).[20-21] Indeed, some of them are being clinically tested for diseases where PP2A activity appears depressed.[22-23] Consequently, the multitarget-directed ligands that we have reported, by blocking VGCC and avoid the PP2A inhibition, elicited neuroprotection in various in vitro models of neurodegeneration, standing out the derivative ITH12657 (1-benzyl-5-methyl-3-(piperidin-1-ylmethyl-1*H*-indole, **2**; Fig. 1).[13] Attempting to optimize its therapeutic strengths, we herein present the evaluation of how aromatic substitution at the pending phenyl ring could modulate the affinity with both VGCC and PP2A, and their consequences over the neuroprotection observed in an experimental model of neuronal damage related to AD.

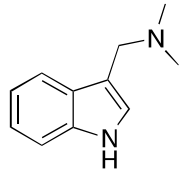

Gramine (**1**)

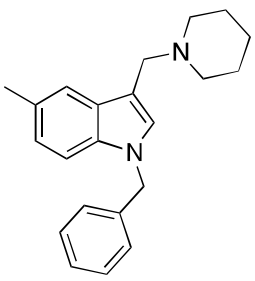

ITH12657 (**2**)

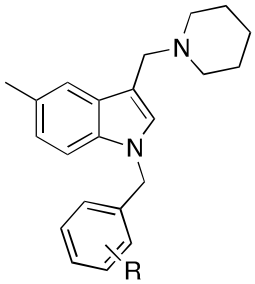

This work

ACCEPTED MANUSCRIPT

Fig. 1. Chemical structures of gramine and the lead compound ITH12657 (**2**),[13] together with the chemical substitution herein proposed.

2. Results and discussion

2.1. Chemistry

We have selected various substituents possessing different steroelectronic behavior that would affect the phenyl ring electronegativity, but also eligible to make hydrogen bonds or to pose into hydrophobic binding pockets within the PP2A. Thus, halogens, methyl group or the highly electron-demanding and polar nitro group, were selected.

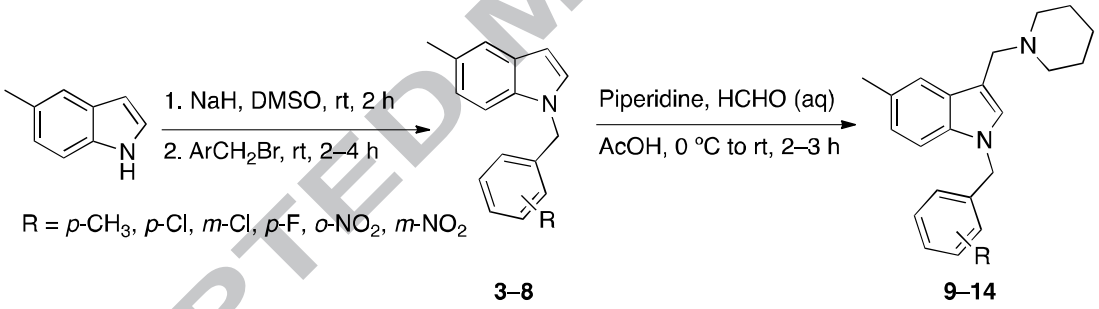

Scheme 1. Synthesis of *N*-benzylated 3-piperidinylmethylgramine derivatives

Functionalization of the indole nitrogen was carried out by deprotonation with NaH in DMSO, followed by addition of the corresponding benzyl bromide bearing the corresponding substitution, furnishing intermediates **3–8** in good yields, except for the reaction to obtain the *o*-nitro derivative (32%), presumably due to the stereo-electronic repulsions with the negative-charged indole amide. Otherwise, the presence of nitro groups provoked reaction crudes with high presence of by-

ACCEPTED MANUSCRIPT

products, likely by alkylation on C3 or C7, which made chromatographic purifications necessary.

Next, a Mannich-type reaction was carried out to prepare the gramine derivatives **9–14** analogues to the head compound **2**. The order of reagents addition was essential to get the best chemical yields, so piperidine and formaldehyde were firstly mixed in glacial acetic acid and stirred for 10 min, to subsequently be added to intermediates **3–8**. It is worthwhile mentioning that 3-aminomethylindoles are sensitive to low pH in aqueous media, undergoing a retro-Mannich transformation that generates 3-methylidenindoles. To avoid such by-reaction, both quenching and extractions were carried out with basic (pH = 14) aqueous phases. Oily products **9–14** were obtained with medium to excellent yields (50–92%). As keys to confirm the full conversion of intermediates into products, the aromatic doublet assigned to H3 disappeared from the crude ^{1}H NMR, along with the rise of a two proton-integrated singlet that corresponded to the new CH_2 bonded to C3. Although nicely dissolved in DMSO, compounds **9–14** presented partial solubility in water (below 0.1 mM). With the goal of enhancing both aqueous solubility and manipulation for the biological assays, they were salinized to their oxalate salts by treatment with oxalic acid 1M in dry ethyl acetate (Supplementary data), obtaining white and powder solids with high yields (72–91%), and improved aqueous solubility (10 mM). The foreseeable protonation at the piperidine nitrogen was confirmed by the low-field shifting of the neighboring C3CH_2 protons (from 3.58 to 4.33 ppm) and the piperidine signals, together with a broadening of the H2” signal.

*2.2. Effect of compounds **9–14** on the neuronal Ca^{2+} overload*

ACCEPTED MANUSCRIPT

We assessed the ability of compounds to minimize altered Ca^{2+} elevations into neurons by two ways. Firstly, warned by the documented pharmacological results of **2** and its analogues,[13] we subjected SH-SY5Y neuroblastoma cells with high K^+ (70 mM), which evokes cell depolarization and VGCC opening.[24] The consequent cytosolic Ca^{2+} ($[Ca^{2+}]_c$) increase was dramatically prevented by compounds **9–14**, pre-incubated at the concentration of 10 μM (Table 1). This huge blockade prompted us to analyze their IC_{50} values, defined as the concentration of compound capable of reducing by 50% the 70 mM K^+-triggered Ca^{2+} entry into SH-SY5Y cells (Fig. 2). Compounds incubated at several concentrations depicted nice dose-response curves, with similar IC_{50} values, between 1.8 and 4.8 μM, though substitutions at *meta* position slightly offered better IC_{50} data. Iwata et al reported closely related gramine derivatives, possessing benzyl substituent at the indole NH, which blocked VGCC in a similar fashion.[25] By electrophysiological experiments, under the patch-clamp whole-cell configuration, we have proposed that this family of gramine derivatives, leaded by **2**, would directly interact to the VGCC ionic channel.[13]

Secondly, keeping our attention on the participation of neuronal Ca^{2+} overload in physiopathological processes driving to neurodegeneration, no one would dispute the participation of NMDA receptors in the progression of AD.[26] Indeed, one of the sole four prescribed drugs for AD is the NMDA receptor blocker memantine.[7] For this reason, we were interested in assessing the blocking effect of compounds **2** and **9–14** on NMDA receptors. To achieve this purpose, we selected a neuronal type that possesses functional NMDA-sensitive glutamate receptors, i.e. the rat cortical embryonic neurons,[27] inducing $[Ca^{2+}]_c$ increase through these channels with NMDA, at the concentration of 10 μM (Table 1).

ACCEPTED MANUSCRIPT

Table 1

Effect of compounds **2** and **9–14**, tested at 10 μM, on the neuronal Ca^{2+} increases induced by either depolarization (70 mM K^+) or NMDA receptors recruitment (NMDA 10 μM),[a] measured with the Ca^{2+}-sensitive fluorescent probe Fluo-4.

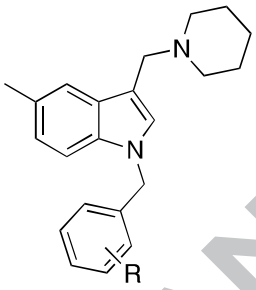

Compounds	R	70 K^{+b}	NMDA[c]
Nifedipine	-	32 ± 6	-
Memantine	-	-	41 ± 14
2	H	87 ± 8	42 ± 3
9	*p*-CH_3	94 ± 1	32 ± 3
10	*m*-Cl	97 ± 1	37 ± 14
11	*p*-Cl	95 ± 3	52 ± 1
12	*p*-F	79 ± 2	34 ± 6
13	*o*-NO_2	90 ± 6	24 ± 16
14	*m*-NO_2	90 ± 4	22 ± 6

[a]Data are expressed as % blockade compared with the control situation [neurons only incubated with vehicle (DMSO 0.1%)], and are means ± SEM of at least four independent experiments in triplicates. [b]SH-SY5Y neuroblastoma cells exposed to high extracellular concentration of KCl (70 mM). [c]Rat cortical embryonic neurons,

ACCEPTED MANUSCRIPT

from two different pregnant rats, stimulated with NMDA 10 μM. Nifedipine[28] and memantine[7] at concentrations of 10 μM were used as standard VGCC and NMDA receptors blockers, respectively. Compounds were tested at the concentration of 10 μM.

The consequent elevation of $[Ca^{2+}]_c$ by the contest of NMDA receptors was slightly reduced by compounds **9–14** preincubated at 10 μM (Table 1), averaging a 30% blockade. Compound **11**, which presents a chlorine atom at *para* position, was the best NMDA receptors blocker, as halved the Ca^{2+} entry at 10 μM (Table 1). Preliminary structure-activity relationships point out that substituents well accommodated into hydrophobic pockets, like alkyl groups or halogens, would favor the blockade of the NMDA-evoked Ca^{2+} entry. Comparing with blockade data from the experiments of depolarization-induced Ca^{2+} entry, compounds **9–14** were much better blockers of VGCC than of NMDA receptors, as **2** and its derivatives halved the 70 K^+-evoked Ca^{2+} entry in SH-SY5Y cells at concentrations around 3 μM (Fig. 2). This differential blockade is consistent with data from literature, where gramine and its derivatives have exerted substantial blockade of VGCC,[25] unlike that reported over NMDA receptors, where gramine did not show blocking activities at higher concentrations.[29]

ACCEPTED MANUSCRIPT

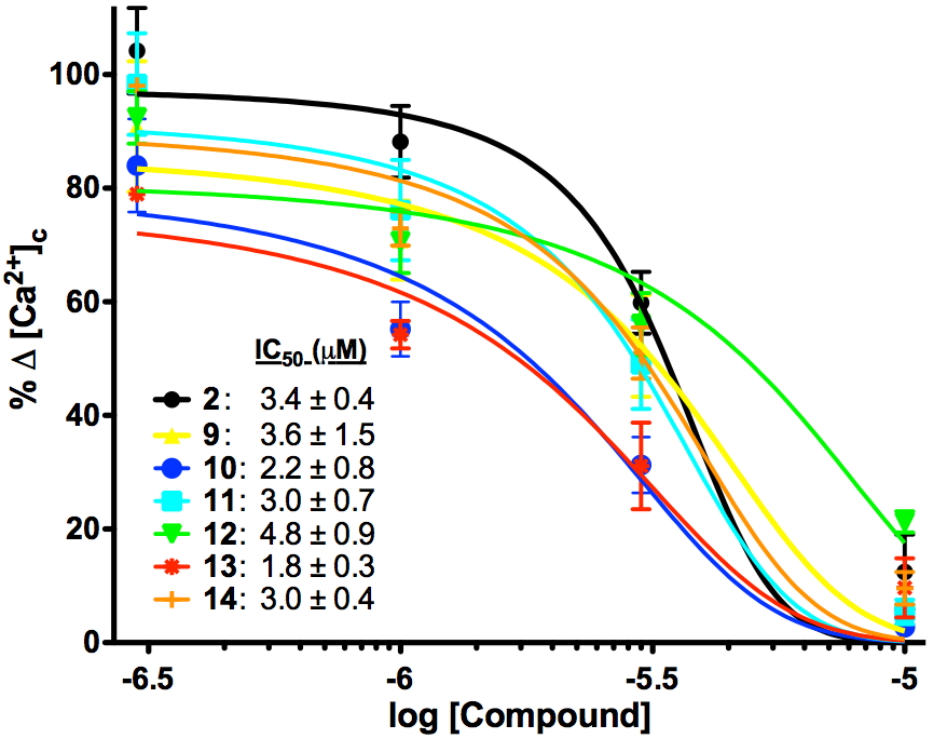

Fig. 2. Dose-response curves of the blockade exerted by compounds **2** (R = H, black line) and **9–14** [R = CH_3 (yellow line), Cl (blue lines), F (green line), NO_2 (reddish lines)] on the cytosolic Ca^{2+} ($[Ca^{2+}]_c$) increases originated by 70 mM K^+-evoked VGCC opening in SH-SY5Y cells. Data points are presented as means ± SEM of three experiments in triplicates. Curves were built under non-linear regression fit with variable slope, of log (compound) *vs* normalized responses respect to the $\Delta[Ca^{2+}]$, obtained from cultures only preincubated with vehicle (DMSO 0.1%). **(COLOR SHOULD BE USED IN PRINT, PLEASE)**

The little blocking effect of compounds **9–14** over NMDA receptors could be due to an indirect interaction, as it has been reported that active PP2A generates a stable complex with NMDA receptors, and thus catalyzing the dephosphorylation of two serines at the NMDA-NR1 subunit. This dephosphorylation desensitizes NMDA

ACCEPTED MANUSCRIPT

receptors, producing a lesser Ca^{2+} influx.[30] Therefore, should compounds **9–14** behaved as PAD, a possibility exists that this activity was responsible of the slight NMDA receptors blockade observed in the Fluo-4-monitored Ca^{2+} entry measurements under NMDA stimulation. To demonstrate the pro-PP2A activity of compounds **9–14**, we conducted phosphatase activity assays in SH-SY5Y cells compromised by the PP2A inhibitor okadaic acid (OA).

*2.3. Effect of compounds **9–14** on the PP2A-performed phosphatase activity*

The inhibition of PP2A performed by OA is a widely used experimental model of AD, due to this polyether toxin causes PP2A dysfunction and thereby causing Tau hyperphosphorylation and further NFT generation.[31] The administration of OA in animal models elicits manifestations of cognitive impairment compatible with AD, such as both short and long-term memory formation,[32] and spatial memory deficits.[33] In addition, people intoxicated with OA, from the intake of dinoflagellates-contaminated seafood, experimented memory losses that were more pronounced in elderly.[34] Hence, the scope of the inhibition of PP2A by OA allows us to analyze the ability of our compounds to recover the phosphatase activity in situations were PP2A is depressed, as those observed in AD. SH-SY5Y cells mainly express the PP2A isoform with the ubiquitously found PR55α B regulatory subunit.[35] Thus, this cell line can be considered a reliable model for appraising the PP2A impairment occurred in AD brains. Applied to SH-SY5Y cells at 15 nM for 18 h (Fig. 3, top), OA did not compromise cell viability, but provoked a noticeably decay of the phosphatase activity by 25 ± 2% (Fig. 3), recorded by the method of *p*-nitrophenol phosphate (*p*NPP), which is a colorimetric dye hydrolyzed by phosphatase

ACCEPTED MANUSCRIPT

enzymes that produce chromogenic (λ = 405 nm) *p*-nitrophenolate in basic environment.. The PP2A activity fall was prevented by the presence of most of the compounds, pre- and co-incubated at 0.1 μM (Fig. 3), standing out the *p*-fluorinated compound **12**, which kept the phosphatase activity of SH-SY5Y cells in a 93 ± 3% comparing with control cells (cells not exposed to OA), which implies a 73% recovery of the PP2A-dependent phosphatase activity comparing with the OA group. Therefore, compounds **9–12**, acting as PADs,[20] improved the effect of the head **2**, confirming that, for this family of **1** derivatives, some substitutions at pending phenyl ring could favor a better fitting into the PP2A binding site. Memantine 10 nM, was used as standard in these experiments, because of its reversal effect in situations of PP2A inhibition.[36]

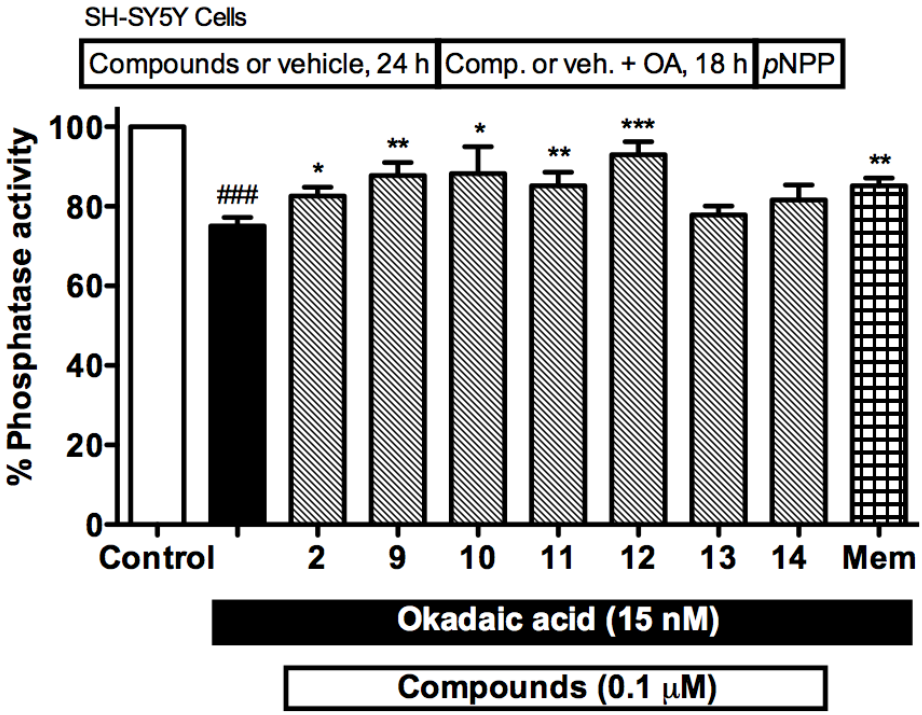

Fig. 3. Effect of compounds **9–14** on the PP2A-leaded phosphatase activity compromised by okadaic acid (OA) in SH-SY5Y cells, measured by the method of

ACCEPTED MANUSCRIPT

the *para*-nitrophenol phosphate (*p*NPP). Data are means ± SEM of at least three independent experiments, normalized over the maximum phosphatase activity (control), obtained from SH-SY5Y cells not exposed to OA. Memantine (Mem) at 10 nM was used as standard in these experiments. $^{###}p < 0.001$, compared with control group (white bar), $^{***}p < 0.001$, $^{**}p < 0.01$, $^{*}p < 0.05$ compared with cells stimulated with OA in absence of compounds (black bar).

2.4 Molecular docking

We hypothesize that compounds **9–14** exert their PAD profile by a direct interaction with PP2A. Computational docking experiments were executed to support this proposal, using the constitutive PP2A AC dimer, deposited in the Protein Data Bank (2IE4, www.rcsb.org).[37] Thus, we predicted the best pose of compound **12** that would explain why it is the best PAD (Fig. 4). The molecular docking revealed several contacts between **12** and various amino acids into the PP2A catalytic subunit C (PP2Ac) unable to hinder the catalysis played by PP2A. It has been documented that the selective inhibitor OA binds PP2Ac in a vast area, where its C1–C12 fragment blocks the hydrolytic site of PP2Ac, as shown in Fig. 4A, and the two spare C19–C27 and C29–C38 fragments only confer affinity and selectivity over PP1, respectively.[38-39] Interestingly, compound **12**, in a slightly different manner to that performed by **2**,[13] bound preferentially to amino acids that also bind fragments the C19–C27 and C–29–C38 fragments of OA (Fig. 4A), highlighting Trp200, together with both Arg214 and Gln122 skeletons, which form a hydrophobic pocket where both indole and the pending phenyl ring of **2** pose (Fig. 4B). His118 illustrates a strong H-bond with the charged nitrogen of the

ACCEPTED MANUSCRIPT

piperidine moiety and, in addition, a weak H-Bond can be appreciated between the skeleton NH of Ile123 and the fluorine atom of **12** (Fig. 4C). Hydrogen bonding with fluorine, despite its weakness, has been detected in several crystal PDB structures, and explains improvements in pharmacodynamic outcomes,[40] as what is found out herein.

(A)

ACCEPTED MANUSCRIPT

ACCEPTED MANUSCRIPT

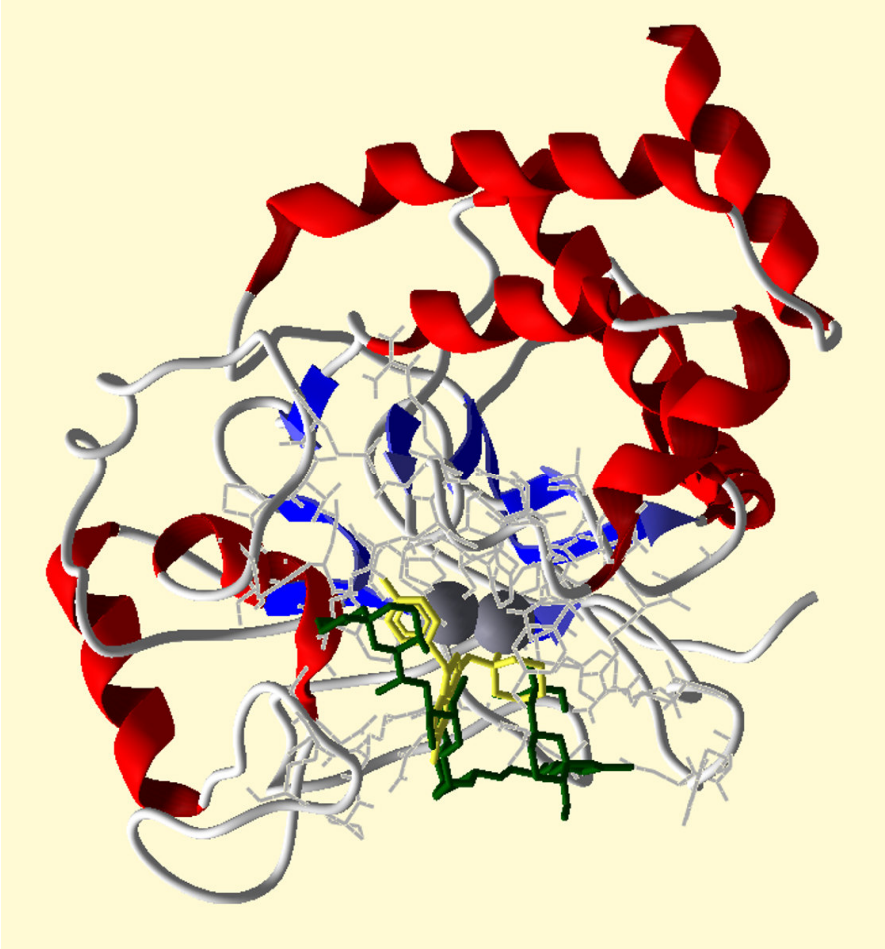

(B)

ACCEPTED MANUSCRIPT

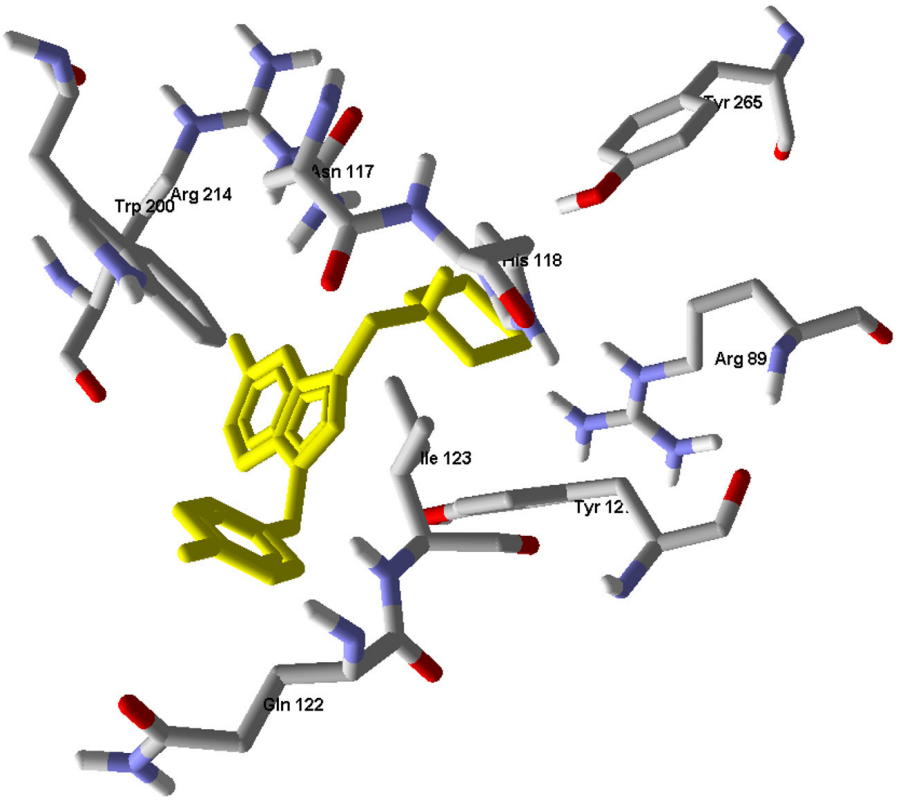

(C)

ACCEPTED MANUSCRIPT

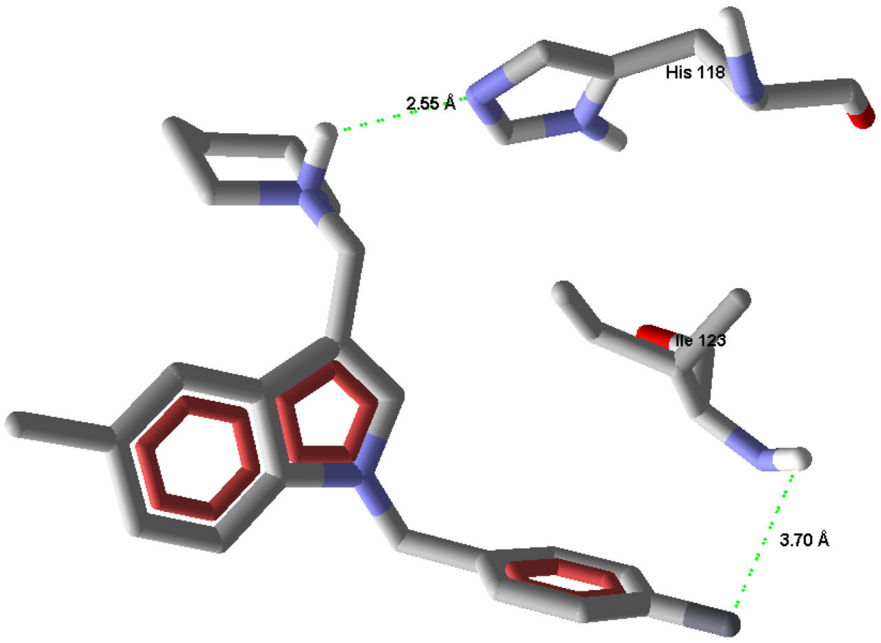

Fig. 4. (**A**) Molecular docking of compound **12** (yellow) within PP2A catalytic subunit (PP2Ac) binding site (main interacting residues and Mn^{2+} ions in gray color), including the pose shaped by OA (green). (**B**) Pose of **12** into the hydrophobic pocket built by Arg214, Gln122, and Trp200. (**C**) Hydrogen bonds between **12** and His118 and Ile123 (energy scores provided in Supplementary Material, Table S1)

2.5. Cell viability experiments

The positive outcomes on the two therapeutic targets aimed, prevention of the neuronal Ca^{2+} overload and reactivation of PP2A, prompted us to assess the neuroprotective potential of compounds **9–14** with a in vitro model of PP2A inhibition. The administration of OA depicts a plethora of physiopathological events beyond the expected Tau hyperphosphorylation and subsequent NFT formation, which collectively contribute to the AD onset. For instance, the PP2A inhibition

ACCEPTED MANUSCRIPT

exacerbated by OA drew Aβ aggregation,[41] activation of several kinases, such as ERK1/2 and PKC,[42] decrease of ACh levels,[33] activation of NMDA receptors,[43] free radical generation,[44] mitochondrial dysfunction,[45] oxidative DNA damage,[46] and sustained activation of VGCC,[47] among others. All of these observations make OA a reliable tool to study neuroprotective drugs addressed to AD. When exposed to SH-SY5Y cells at the concentration of 20 nM for 20 h, OA substantially diminished the cell viability by 50.1 ± 0.2 % respect to that of untreated cells. In this scenario, the pre- and co-administration of compounds **9–14** (0.1 μM) mitigated this decrease in a very similar manner, augmenting the SH-SY5Y cells viability by about 67%. The *o*-nitro-derivate **13** the best neuroprotectant of the family, as it elevated cell viability to 70 ± 3%, what supposes a recovery of 40%. Otherwise, none of the compounds overcame the cell viability of OA-challenged cells incubated with compound **2** (73 ± 3%). Memantine was used as reference compound due to its confirmed neuroprotective efficacy in situations of PP2A depression.[36]

ACCEPTED MANUSCRIPT

ACCEPTED MANUSCRIPT

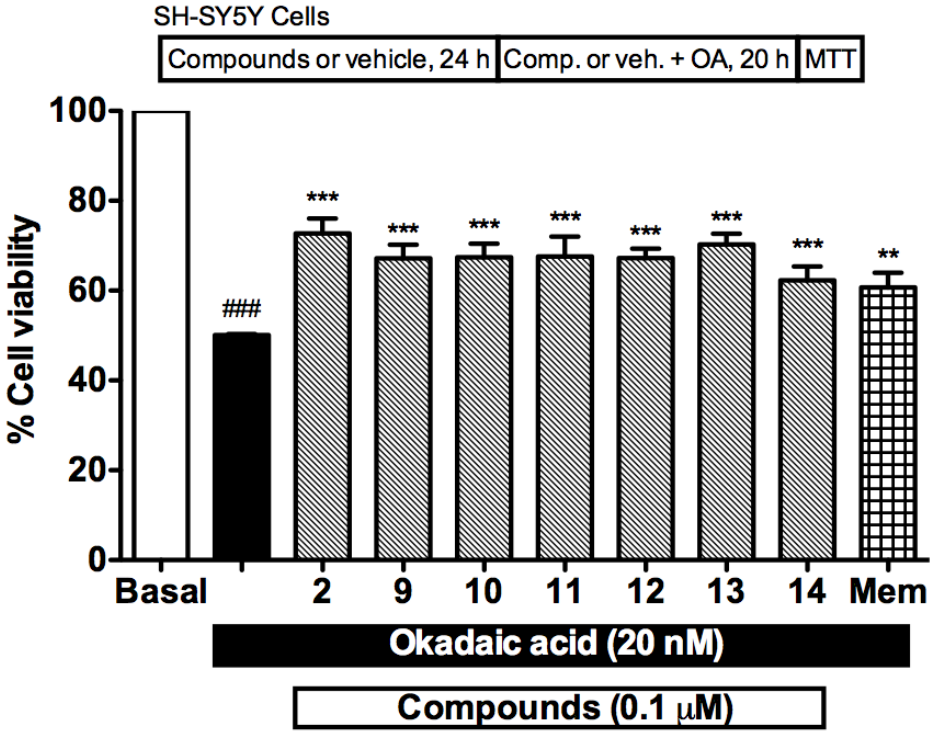

Fig. 5. Effect of compounds **2** and **9–14** on the cell viability challenged by OA at 20 nM in SH-SY5Y cells, measured by the method of the MTT reduction. Data are means ± SEM of four independent experiments, and expressed as % cell viability, normalized respect to the cell viability of SH-SY5Y cells non-incubated with OA nor compounds. Memantine (Mem) at 10 nM was used as standard in these experiments. $^{###}p < 0.001$, compared with basal group (white bar), $^{***}p < 0.001$, $^{**}p < 0.01$, compared with cells exposed to OA in absence of compounds (black bar).

Likewise, an additional feature to take into account is the possible toxicity by themselves. Thus, compounds **9–14** *per se* exposed to SH-SY5Y cells at 3 μM, a 30-fold higher concentration than the used in neuroprotection assays, did not diminished the cell viability (Fig. S1, supplementary data), which was only compromised from 10 μM, underlining chlorinated derivatives **10** and **11.**

ACCEPTED MANUSCRIPT

Conversely, the fluorinated derivative **12** scarcely reduced cell viability at 10 μM, in a non-statistically significant fashion.

3. Conclusions

In summary, we have studied the influence of the chemical substitution at the pending phenyl ring over the pharmacological properties of *N*-benzylgramine derivatives studied as neuroprotectants, regarding to their modulating effect on both PP2A and cell Ca^{2+} overload, demonstrating that these activities can be modified depending on the substituent selected. Nitro groups at the phenyl achieved neuroprotection in this series by enhancing VGCC blockade, while fluorine improved the recovery of the PP2A-conducted phosphatase activity. Chlorine atoms provided derivatives with good pharmacological activities in all the assays, but dramatically damaged SH-SY5Y cells at 10 μM (Fig. S1) and therefore, though presenting a high therapeutic index, their further preclinical appraisal, as well as the preparation of new chlorinated **2** derivatives, are not advisable. On the other hand, regarding to the neuroprotective assays, despite there are not significant differences among all the analyzed compounds, the facts that compound **12**, the best PAD of the family, was not the best neuroprotectant, and the good neuroprotective actions of **13**, which was unable to prevent the inhibitory actions of OA PP2A, should indicate us that neuroprotection against a model of PP2A impairment can be achieved downstream, where other biological targets, such as VGCC or NMDA receptors, are recruited. This can be considered an accolade to the multitarget-directed ligands strategy, pointing out that

ACCEPTED MANUSCRIPT

pharmacological actions by neuroprotectants over different biological targets should bear in mind to accurately describe drug mechanisms of action.

The derivative **12**, which possesses a hydrogen-isosteric fluorine atom at *para* position of the phenyl ring, is presumably the most stable against the CYP-performed *para*-oxidation. Moreover, it showed the less toxicity of the family, measured as cell viability of SH-SY5Y cells exposed to compounds for 48 h, being compound **12** non-toxic at 100-fold concentrations than those where it protected against OA neurotoxicity and PP2A inhibition. Once evaluated, compound **12** seems to be the most optimal candidate for further preclinical studies by its good down-regulating effect over cell Ca^{2+} overload, excellent recovery of the OA-inhibited PP2A activity, and lack of toxicity at high concentrations, together with a promising neuroprotective profile.

4. Materials and methods

4.1. General

5-methylindole, NaH, selected arylmethyl bromides, piperidine, 37% aqueous formaldehyde, OA sodium salt, memantine, KCl, nifedipine, the colorimetric dye MTT, melatonin, glutamate, and reagents for SH-SY5Y cells culture, were purchased from Merck (Madrid, Spain). Acetic acid was purchased from Alfa-Aesar (Karlsruhe, Germany). Sodium sulfate was purchased from LabKhem (Mataró, Spain). Kit for the determination of phosphatase activity (*p*NPP assay) and solvents used for syntheses, isolation, and chromatographic separations, with analytical grade, were purchased from VWR (Barcelona, Spain) and, when used for the preparation of final compounds, neutralized from acid traces with basic

ACCEPTED MANUSCRIPT

alumina (Merck, Madrid, Spain). Fluorescent dye Fluo-4/AM and reagents for rat cortical neurons culture were purchased from Life Technologies (Alcobendas, Spain). Reactions were monitored with TLC at 254 nm UV light, using silica gel (60 Å) as stationary phase for the *N*-alkylation, and basic alumina (60 Å) for the Mannich-type reaction, both purchased from Merck. Reactions were carried out in glassware systems purged from air with vacuum/argon cycles and run under Ar atmosphere. When necessary, chromatographic purifications were carried out with automatized flash chromatographic station (Biotage, Uppsala, Sweden), using pre-charged columns. Melting points were obtained with a Stuart SMP-10 apparatus (Staffordshire, UK), without correction. IR spectrum was obtained in a Bruker IFS60v FTIR spectrophotometer. MS spectra were acquired in an ABSciex QSTAR spectrometer under the high-resolution configuration with electrospray as ionization source. ^{1}H and ^{13}C NMR spectra were acquired in a Bruker AVANCE 300 MHz station (corresponding to a 75.4 MHz for the ^{13}C detection), expressed as ppm, and calibrated upon the residual proton signal from deuterated solvents. Purity of final compounds was confirmed by elemental analysis in a LECO CHNS-932 station.

4.2. General procedure for the N*-alkylation of 5-methyl-1*H*-indole*

Following an experimental procedure recently described,[13] NaH (1.2 equiv, 60% in mineral oil) was added to a solution of 5-methyl-1*H*-indole (1 equiv) in DMSO (5 mL/mmol) and stirred at rt for 2 h. Afterwards, the corresponding arylmethyl bromide (1.2 equiv) was injected to the reaction mixture, which was stirred at rt for several hours up to no significant evolution of the reaction or the complete disappearance of substrate. Reaction was quenched by addition of water (10 mL/mmlol) and extracted with CH_2Cl_2 (3 × 30 mL/mmol), dried (Na_2SO_4), filtered,

ACCEPTED MANUSCRIPT

and evaporated. When necessary, the crude was purified with automatized flash chromatography, yielding pure intermediates with spectral data according to their structure.

*4.3. 5-methyl-1-(4-methylbenzyl)-1*H*-indole (**3**)*

Following the *general procedure 4.2*, 5-methyl-1*H*-indole (200 mg, 1.52 mmol) [NaH 60% in mineral oil (74 mg, 1.83 mmol), 4-methylbenzyl bromide (338 mg, 1.83 mmol)] yielded **3** (299 mg, 84%). ^{1}H NMR ($CDCl_3$, 300 MHz) δ 7.46 (bs, 1H, H4), 7.20 (d, 1H, $J_{6\text{-}7}$ = 8.4 Hz, H7), 7.13–7.01 (m, 6H, Ar), 6.48 (d, 1H, $J_{2\text{-}3}$ = 3.3 Hz, H3), 5.27 (s, 2H, CH_2), 2.47 (s, 3H, C5CH_3), 2,33 (s, 3H, C4'CH_3).

*4.4. 1-(3-chlorobenzyl)-5-methyl-1*H*-indole (**4**)*

Following the *general procedure 4.2*, 5-methyl-1*H*-indole (200 mg, 1.52 mmol) [NaH 60% in mineral oil (74 mg, 1.83 mmol), 3-chlorobenzyl bromide (388 mg, 1.83 mmol)] yielded **4** (318 mg, 82%). ^{1}H NMR ($CDCl_3$, 300 MHz) δ 7.51 (bd, 1H, H4), 7.32–6.99 (m, 7H, Ar), 6.55 (bd, 1H, H3), 5.32 (s, 2H, CH_2), 2.52 (s, 3H, CH_3).

*4.5. 1-(4-chlorobenzyl)-5-methyl-1*H*-indole (**5**)*

Following the *general procedure 4.2*, 5-methyl-1*H*-indole (200 mg, 1.52 mmol) [NaH 60% in mineral oil (74 mg, 1.83 mmol), 4-chlorobenzyl bromide (388 mg, 1.83 mmol)] yielded **5** (258 mg, 66%). ^{1}H NMR ($CDCl_3$, 300 MHz) δ 7.55 (bd, 1H, H4), 7.32 (d, 2H, $J_{2'\text{-}3'}$ = 8.4, H3', H5'), 7.20 (d, 1H, $J_{6\text{-}7}$ = 8.1, H7), 7.14–7.10 (m,

ACCEPTED MANUSCRIPT

2H, H6, H2), 7.06 (d, 2H, $J_{2'-3'}$ = 8.4, H2', H6'), 6.58 (d, 1H, J_{2-3} = 3.0 Hz, H3), 5.28 (s, 2H, CH_2), 2,55 (s, 3H, CH_3).

*4.6. 1-(4-fluorobenzyl)-5-methyl-1*H*-indole (**6**)*

Following the *general procedure 4.2*, 5-methyl-1*H*-indole (200 mg, 1.52 mmol) [NaH 60% in mineral oil (74 mg, 1.83 mmol), 4-fluorobenzyl bromide (346 mg, 1.83 mmol)] yielded **6** (256 mg, 70%). ^{1}H NMR ($CDCl_3$, 300 MHz) δ 7.44 (bs, 1H, H4), 7.15 (d, 1H, J_{6-7} = 8.4, H7), 7.09–6.94 (m, 6H, Ar), 6.48 (bd, 1H, J_{2-3} = 3.0 Hz, H3), 5.25 (s, 2H, CH_2), 2.45 (s, 3H, CH_3).

*4.7. 5-methyl-1-(2-nitrobenzyl)-1*H*-indole (**7**)*

Following the *general procedure 4.2*, 5-methyl-1*H*-indole (200 mg, 1.52 mmol) [NaH 60% in mineral oil (74 mg, 1.83 mmol), 2-nitrobenzyl bromide (395 mg, 1.83 mmol)] yielded **7** (131 mg, 32%). ^{1}H NMR ($CDCl_3$, 300 MHz) δ 8.17 (m, 1H, H3'), 7.48 (s, 1H, H4), 7.40 (m, 2H, Ar), 7.11 (d, 1H, J_{2-3} = 3.0 Hz, H2), 7.02 (m, 2H, Ar), 6.56 (d, 1H, J_{2-3} = 3.0 Hz, H3), 6.47 (m, 1H, H5'),5.74 (s, 2H, CH_2), 2.46 (s, 3H, CH_3).

*4.8. 5-methyl-1-(3-nitrobenzyl)-1*H*-indole (**8**)*

Following the *general procedure 4.2*, 5-methyl-1*H*-indole (200 mg, 1.52 mmol) [NaH 60% in mineral oil (74 mg, 1.83 mmol), 3-nitrobenzyl bromide (395 mg, 1.83 mmol)] yielded **8** (264 mg, 65%). ^{1}H NMR ($CDCl_3$, 300 MHz) δ 8.11 (d, 1H, $J_{5'-6'}$ =

ACCEPTED MANUSCRIPT

6.3 Hz, H4'), 8.04 (s, 1H, H2'), 7.49–7.42 (m, 2H, H4, H5'), 7.31 (bd, 1H, $J_{6'-5'}$ = 7.8 Hz, H6'), 7,12–7,08 (m, 2H, H2, H7), 7.01 (bd, 1H, J_{6-7} = 8.7, H6), 6.53 (d, 1H, J_{2-3} = 3,3 Hz, H3), 5.39 (s, 2H, CH_2), 2,45 (s, 3H, CH_3).

*4.9. General procedure for the synthesis of 1-arylmethyl-5-methyl-3-(piperidin-1-methyl)-1*H*-indoles* ***9–14***

Following an experimental procedure recently described,[13] piperidine (1 equiv) and formaldehyde (37%$_{aq}$, 1 equiv) were stirred in glacial acetic acid (3 mL/mmol) for 10 min. Then, this mixture was added to an ice-cold, round-bottomed flask with the corresponding intermediate **3**–**8** (1 equiv). The reaction mixture was stirred at 0 º C for 5 min, then at rt for several hours until the reaction was complete (TLC). Reaction was quenched by addition of NaOH (30%$_{aq}$) up to pH 14, extracted with neutralized CH_2Cl_2 (3 × 30 mL/mmol), dried (anh. Na_2SO_4), filtered, and evaporated to get compounds **9–14** as yellowish oils, which did not require further chromatographic purification in most of the cases. Compounds **9–14** were dissolved in dry ethyl acetate (10 mL/ mmol) under inert atmosphere, and a solution of oxalic acid (1 equiv, 1M in dry ethyl acetate) was dropwisely injected. Salinization was allowed to proceed for 2 h and the fine white precipitate formed was isolated by centrifugation (10 min, 750 rpm) accompanied by dry ethyl acetate wash-ups. Traces of ethyl acetate were removed by vacuum. Oxalate salts of compounds **9–14** showed spectral and analytical data according to their structure.

*4.10. 5-methyl-1-(4-methylbenzyl)-3-(piperidin-1-ylmethyl)-1*H*-indole (**9**)*

ACCEPTED MANUSCRIPT

Following the *general procedure 4.9*, reaction of **3** (150 mg, 0.64 mmol) [piperidine (54 mg, 0.64 mmol), formaldehyde (30%$_{aq}$, 47 µL, 0.64 mmol)] yielded **9** (195 mg, 92%) as a yellow oil that did not need further chromatographic purification. ^{1}H NMR (acetone-d_6, 300 MHz) δ 7.49 (s, 1H, H4), 7.22 (d, 1H, $J_{6\text{-}7}$ = 8.4 Hz, H7), 7.17 (s, 1H, H2), 7.11–7.05 (AA'BB', 4H, H2', H3'), 6.91 (dd, 1H, $J_{6\text{-}7}$ = 8.4 Hz, $J_{4\text{-}6}$ = 1.5 Hz, H6), 5.30 (s, 2H, N1CH_2C1'), 3.58 (s, 2H, C3CH_2), 2.38 (m, 7H, H2'', C5CH_3), 2.26 (s, 3H, C4'CH_3), 1.50 (m, 4H, H3''), 1.40 (m, 2H, H4''). Its oxalate salt was prepared following the procedure described in *4.9*. Compound **9** (178 mg, 0.54 mmol) [oxalic acid 1M (49 mg, 0.54 mmol)] yielded its oxalate salt as a white solid (142 mg, 73%). Mp 178–180 ºC; ^{1}H NMR (DMSO-d_6, 300 MHz) δ 7.60 (s, 1H, H4), 7.54 (s, 1H, H2), 7.36 (d, 1H, $J_{6\text{-}7}$ = 8.4 Hz, H7), 7.10 (s, 4H, H2', H3'), 6.99 (d, 1H, $J_{6\text{-}7}$ = 8.4 Hz, H6), 5.34 (s, 2H, N1CH_2C1'), 4.33 (s, 2H, C3CH_2), 3.08 (m, 4H, H2''), 2.38 (s, 3H, C5CH_3), 2.23 (s, 3H, C4'CH_3), 1.70 (m, 4H, H3''), 1.48 (m, 2H, H4''); ^{13}C NMR (DMSO-d_6, 75.4 MHz) δ 164.7, 136.8, 134.8, 134.3, 132.0, 129.2, 128.8, 128.5, 127.2, 123.6, 118.5, 110.5, 102.3, 51.3, 50.6, 49.2, 22.7, 21.6, 21.3, 20.7; IR (KBr) ν 2920, 1630, 1380, 1176, 730 cm^{-1}; HRMS (API-ES) m/z (M^+) calcd. for $C_{23}H_{29}N_2$ 333.2325, found, 333.2340 (± 4.5 ppm). Anal. $C_{23}H_{28}N_2 \cdot C_2O_4H_2 \cdot 1/2\ H_2O$ (C, H, N).

*4.11. 1-(3-chlorobenzyl)-5-methyl-3-(piperidin-1-ylmethyl)-1*H*-indole (**10**)*

Following the *general procedure 4.9*, reaction of **4** (150 mg, 0.59 mmol) [piperidine (50 mg, 0.59 mmol), formaldehyde (30%$_{aq}$, 44 µL, 0.59 mmol)] yielded **10**, which was purified by basic alumina flash chromatography with ethyl acetate/hexane mixtures as eluent, obtaining a yellow oil (195 mg, 76%). ^{1}H NMR (acetone-d_6, 300

ACCEPTED MANUSCRIPT

MHz) δ 7.52 (bs, 1H, H4), 7.34–7.27 (m, 2H, Ar), 7.23–7.21 (m, 2H, Ar), 7.12 (m, 2H, Ar), 6.94 (dd, 1H, $J_{6\text{-}7}$ = 8.4, $J_{4\text{-}6}$ = 1.2 Hz, H6), 5.40 (s, 2H, N1CH_2C1'), 3.60 (s, 2H, C3CH_2), 2.39 (m, 7H, H2'', CH_3), 1.52 (m, 4H, H3''), 1.41 (m, 2H, H4''). Its oxalate salt was prepared following the procedure described in *4.9*. Compound **10** (40 mg, 0.11 mmol) [oxalic acid 1M (10 mg, 0.11 mmol)] yielded its oxalate salt as a white solid (42 mg, 84%). Mp 175–177 ºC; ^{1}H NMR (DMSO-d_6, 300 MHz) δ 7.65 (s, 1H, H4), 7.57 (s, 1H, H2), 7.39 (m, 1H, H5'), 7.34 (m, 2H, H7, H4'), 7.22 (s, 1H, H2'), 7.14 (bd, 1H, $J_{6'\text{-}7'}$ = 6.5 Hz, H6'), 7.02 (bd, 1H, $J_{6\text{-}7}$ = 8.4 Hz, H6), 5.45 (s, 2H, N1CH_2C1'), 4.35 (s, 2H, C3CH_2), 3.09 (bs, 4H, H2''), 2.39 (s, 3H, CH_3), 1.71 (m, 4H, H3''), 1.49 (m, 2H, H4''); ^{13}C NMR (DMSO-d_6, 75.4 MHz) δ 164.3, 140.5, 140.5, 134.3, 133.2, 131.9, 130.5, 128.9, 128.4, 127.4, 126.8, 125.7, 123.7, 118.6, 110.3, 51.4, 50.5, 48.6, 22.7, 21.5, 21.2; HRMS (API-ES) m/z (M^+) calcd. for $C_{22}H_{26}N_2Cl$ 353.1779, found, 353.1787 (± 2.3 ppm). Anal. $C_{22}H_{25}N_2Cl{\cdot}C_2O_4H_2$ (C, H, N).

*4.12. 1-(4-chlorobenzyl)-5-methyl-3-(piperidin-1-ylmethyl)-1*H*-indole (**11**)*

Following the *general procedure 4.9*, reaction of **5** (150 mg, 0.59 mmol) [piperidine (50 mg, 0.59 mmol), formaldehyde (30%$_{aq}$, 44 μL, 0.59 mmol)] yielded **11**, which was purified by basic alumina flash chromatography with ethyl acetate/hexane mixtures as eluent, obtaining a yellow oil (162 mg, 78%). ^{1}H NMR (acetone-d_6, 300 MHz) δ 7.52 (s, 1H, H4), 7.31 (d, 2H, H2'), 7.21–7.14 (m, 4H, H2, H7, H3'), 6.93 (bd, 1H, $J_{6\text{-}7}$ = 8.4 Hz, H6, 5.34 (s, 2H, N1CH_2C1'), 3.59 (s, 2H, C3CH_2), 2.39 (m, 7H, H2'', CH_3), 1.52 (m, 4H, H3''), 1.41 (m, 2H, H4''). Its oxalate salt was prepared following the procedure described in *4.9*. Compound **11** (114 mg, 0.32 mmol) [oxalic acid 1M (29 mg, 0.32 mmol)] yielded its oxalate salt as a white solid (115

ACCEPTED MANUSCRIPT

mg, 81%). Mp 174–176 ºC; ^{1}H NMR (DMSO-d_6, 300 MHz) δ 7.63 (s, 1H, H4), 7.55 (s, 1H, H2), 7.36 (m, 3H, H2', H7), 7.20 (d, 2H, $J_{2'-3'}$ = 8.4 Hz, H3'), 6.99 (bd, 1H, J_{6-7} = 8.6 Hz, H6), 5.41 (s, 2H, N1CH_2C1'), 4.34 (s, 2H, C3CH_2), 3.09 (bs, 4H, H2''), 2.38 (s, 3H, CH_3), 1.70 (m, 4H, H3''), 1.49 (m, 2H, H4''); ^{13}C NMR (DMSO-d_6, 75.4 MHz) δ 164.7, 136.9, 134.3, 132.1, 132.0, 129.0, 128.9, 128.6, 128.5, 123.7, 118.6, 110.4, 102.5, 51.3, 50.5, 48.6, 22.6, 21.5, 21.2; HRMS (API-ES) m/z (M^+) calcd. for $C_{22}H_{26}N_2Cl$ 353.1779, found, 353.1788 (± 2.5 ppm). Anal. $C_{22}H_{25}N_2Cl{\cdot}C_2O_4H_2{\cdot}1/2H_2O$ (C, H, N).

*4.13. 1-(4-fluorobenzyl)-5-methyl-3-(piperidin-1-ylmethyl)-1*H*-indole (**12**)*

Following the *general procedure 4.9*, reaction of **6** (177 mg, 0.74 mmol) [piperidine (63 mg, 0.74 mmol), formaldehyde (30%$_{aq}$, 55 μL, 0.74 mmol)] yielded **12**, which was purified by basic alumina flash chromatography with ethyl acetate/hexane mixtures as eluent, obtaining a yellow oil (150 mg, 60%). ^{1}H NMR (acetone-d_6, 300 MHz) δ 7.51 (bs, 1H, H4), 7.22–7.18 (m, 4H, H2', H7, H2), 7.07–7.01 (m, 2H, H3'), 6.93 (bd, 1H, J_{6-7} = 8.4 Hz, H6), 5.33 (s, 2H, N1CH_2C1'), 3.58 (s, 2H, C3CH_2), 2.38 (m, 7H, H2'', CH_3), 1.51 (m, 4H, H3''), 1.41 (m, 2H, H4''). Its oxalate salt was prepared following the procedure described in *4.9*. Compound **12** (119 mg, 0.34 mmol) [oxalic acid 1M (30 mg, 0.34 mmol)] yielded its oxalate salt as a white solid (107 mg, 72%). Mp 107–109 ºC; ^{1}H NMR (DMSO-d_6, 300 MHz) δ 7.63 (s, 1H, H4), 7.56 (s, 1H, H2), 7.38 (d, 1H, J_{6-7} = 8.4 Hz, H7), 7.28–7.23 (dd, 2H, $J_{2'-F}$ = 5.6 Hz, $J_{2'-3'}$ = 8.6 Hz, H2'), 7.14 (m, 2H, H3'), 7.00 (bd, 1H, J_{6-7} = 8.4 Hz, H6), 5.40 (s, 2H, N1CH_2C1'), 4.35 (s, 2H, C3CH_2), 3.10 (bs, 4H, H2''), 2.39 (s, 3H, CH_3), 1.71 (m, 4H, H3''), 1.46 (m, 2H, H4''); ^{13}C NMR (DMSO-d_6, 75.4 MHz) δ 164.4, 134.2, 134.0,

ACCEPTED MANUSCRIPT

133.0 ($J_{C1'-F}$ = 174.6 Hz), 131.9, 129.2 ($J_{C2'-F}$ = 8.3 Hz), 128.8, 128.4, 123.6, 118.5, 115.4 ($J_{C3'-F}$ = 21.4 Hz), 110.4, 102.3, 51.2, 50.4, 48.5, 22.5, 21.4, 21.2; HRMS (API-ES) m/z (M^+) calcd. for $C_{22}H_{26}N_2F$ 337.2075, found, 337.2080 (± 1.5 ppm). Anal. $C_{22}H_{25}N_2F{\cdot}C_2O_4H_2{\cdot}1/2H_2O$ (C, H, N).

*4.14. 5-methyl-1-(2-nitrobenzyl)-3-(piperidin-1-ylmethyl)-1*H*-indole (**13**)*

Following the *general procedure 4.9*, reaction of **7** (125 mg, 0.47 mmol) [piperidine (40 mg, 0.47 mmol), formaldehyde (30%$_{aq}$, 35 µL, 0.47 mmol)] yielded **13** (149 mg, 87%) as a yellow oil that did not need further chromatographic purification. ^{1}H NMR (acetone-d_6, 300 MHz) δ 8.15 (m, 1H, H3'), 7.56–7.50 (m, 3H, Ar), 7.21–7.16 (m, 2H, Ar), 6.94 (bd, 1H, J_{6-7} = 8.4, H6), 6.52 (m, 1H, H6'), 5.79 (s, 2H, N1CH_2C1'), 3.62 (s, 2H, C3CH_2), 2.39 (m, 7H, H2'', CH_3), 1.53 (m, 4H, H3''), 1.41 (m, 2H, H4''). Its oxalate salt was prepared following the procedure described in *4.9*. Compound **13** (149 mg, 0.41 mmol) [oxalic acid 1M (37 mg, 0.41 mmol)] yielded its oxalate salt as a white solid (134 mg, 72%). Mp 206–210 ºC; ^{1}H NMR (DMSO-d_6, 300 MHz) δ 8.15 (bd, 1H, $J_{3'-4'}$ = 7.1 Hz, H3'), 7.59 (m, 4H, H2, H4, H4', H5'), 7.29 (d, 1H, J_{6-7} = 8.4, H7), 6.98 (d, 1H, J_{6-7} = 8.4 Hz, H6), 6.52 (bd, 1H, $J_{5'-6'}$ = 7.0 Hz, H6'), 5.82 (s, 2H, N1CH_2C1'), 4.39 (s, 2H, C3CH_2), 2.99 (bs, 4H, H2''), 2.40 (s, 3H, CH_3), 1.72 (m, 4H, H3''), 1.53 (m, 2H, H4''); ^{13}C NMR (DMSO-d_6, 75.4 MHz) δ 164.6, 147.3, 134.6, 134.3, 133.6, 132.5, 129.3, 128.9, 128.4, 128.2, 125.2, 124.0, 118.8, 110.5, 102.9, 51.3, 50.4, 47.0, 22.7, 21.5, 21.3; HRMS (API-ES) m/z (M^+) calcd. for $C_{22}H_{26}N_3O_2$ 364.2020, found, 364.2020 (± 0.0 ppm). Anal. $C_{22}H_{25}N_3O_2{\cdot}C_2O_4H_2{\cdot}1/2H_2O$ (C, H, N).

ACCEPTED MANUSCRIPT

*4.15. 5-methyl-1-(3-nitrobenzyl)-3-(piperidin-1-ylmethyl)-1*H*-indole (**14**)*

Following the *general procedure 4.9*, reaction of **8** (132 mg, 0.50 mmol) [piperidine (42 mg, 0.50 mmol), formaldehyde (30%$_{aq}$, 37 μL, 0.50 mmol)] yielded **14**, which was purified by basic alumina flash chromatography with ethyl acetate/hexane mixtures as eluent, obtaining a yellow oil (91 mg, 50%). ^{1}H NMR (acetone-d_6, 300 MHz) δ 8.11 (m, 1H, H3'), 7.99 (bs, 1H, H2'), 7.58–7.54 (m, 3H, H4, H5', H6'), 7.28 (s, 1H, H2), 7.23 (d, 1H, $J_{6\text{-}7}$ = 8.4 Hz, H7), 6.95 (bd, 1H, $J_{6\text{-}7}$ = 8.4, H6), 5.55 (s, 2H, N1CH_2C1'), 3.61 (s, 2H, C3CH_2), 2.39 (m, 7H, H2'', CH_3), 1.52 (m, 4H, H3''), 1.42 (m, 2H, H4''). Its oxalate salt was prepared following the procedure described in *4.9*. Compound **14** (88 mg, 0.24 mmol) [oxalic acid 1M (22 mg, 0.24 mmol)] yielded its oxalate salt as a white solid (100 mg, 91%). Mp 168–170 ºC; ^{1}H NMR (DMSO-d_6, 300 MHz) δ 8.11 (m, 1H, H4'), 7.97 (s, 1H, H2'), 7.71 (s, 1H, H4), 7.63–7.58 (m, 3H, H2, H5', H6'), 7.40 (d, 1H, $J_{6\text{-}7}$ = 8.4, H7), 7.01 (d, 1H, $J_{6\text{-}7}$ = 8.4 Hz, H6),5.60 (s, 2H, N1CH_2C1'), 4.36 (s, 2H, C3CH_2), 3.10 (bs, 4H, H2''), 2.38 (s, 3H, CH_3), 1.71 (m, 4H, H3''), 1.48 (m, 2H, H4''); ^{13}C NMR (DMSO-d_6, 75.4 MHz) δ 164.7, 148.0, 140.4, 134.3, 133.7, 132.1, 130.3, 129.1, 128.5, 123.9, 122.5, 121.4, 118.7, 110.3, 103.0, 51.3, 50.4, 48.4, 22.7, 21.5, 21.2; HRMS (API-ES) m/z (M^+) calcd. for $C_{22}H_{26}N_3O_2$ 364.2020, found, 364.2027 (± 1.9 ppm). Anal. $C_{22}H_{25}N_3O_2 \cdot C_2O_4H_2 \cdot 1/2H_2O$ (C, H, N).

4.16. Experimental use of animals

The maximum efforts were made to reduce the number of pregnant rats sacrificed for culturing cortical embryonic neurons and their suffering, following the

ACCEPTED MANUSCRIPT

guidelines of the EU Council Directive. Experiments were approved by the Ethics Committee of the Universidad Autonoma de Madrid.

4.17. Cell Cultures

The neuroblastoma SH-SY5Y cell line was obtained from the American Type Culture Collection (ATCC-CRL-2266), maintained and cultured in a 1:1 mixture of MEM and F12 media with 10% of fetal bovine serum (FBS), according to procedures previously described.[12] For fluorescence-based $[Ca^{2+}]_c$ measurements, SH-SY5Y cells were seeded in clear-bottomed, 96-well black plates at a density of 40,000 cells/well, according to a recently described protocol.[13] For viability and phosphatase activity assays, SH-SY5Y cells were seeded in 48-well plates at a density of 70,000 cells/well following the procedure recently reported.[13] Rat cortical embryonic neurons were prepared from 18 days–old embryos, cultured in clear-bottomed, 96-well black plates for the further fluorescence-based $[Ca^{2+}]_c$ measurements at a density of 30,000 cells/well, according to what has been recently described.[48] All the biological assays were conducted in sterile conditions.

4.18. Effect of compounds over the neuronal Ca^{2+} increases

To assess the blocking effect of compounds on the VGCC, we used SH-SY5Y cells charged with the Ca^{2+}-sensitive fluorescent dye Fluo-4/AM at 10 μM in Krebs-HEPES buffer, following a protocol recently described.[13] Compounds were incubated at the desired concentrations, and the Ca^{2+} entry was favored by addition of K^+ 70 mM to the extracellular medium. To evaluate the blocking effect of compounds on NMDA receptors, we have followed a protocol recently reported

ACCEPTED MANUSCRIPT

by our research group.[48] Rat cortical neurons were charged with Fluo-4/AM at 3 μM in Krebs-HEPES buffer and compounds incubated at the concentration of 10 μM. To stimulate Ca^{2+} entry through the NMDA-sensitive glutamate receptors, NMDA was applied at 10 μM. In both cases, fluorescence oscillations as result of the $[Ca^{2+}]_c$ increases were real-time monitored in a multi-well fluorescence plate reader (FluoStar Optima, BMG, Germany), with excitation and emission wavelengths of 485 and 520 nm, respectively. Data were calculated as fluorescence increase (ΔF), according to the formula: $\Delta F = (F_x - F_0)/(F_{max} - F_{min})$, where F_x is the maximum fluorescence obtained after Ca^{2+} entry stimulation, F_0 is the averaged fluorescence before, F_{max} is the maximum fluorescence of the well obtained by treating cells with 5% Triton X-100, and the F_{min} is the minimum fluorescence of well obtained by adding $MnCl_2$ 1 M to the previously Triton-lysed cells. The ΔF data were normalized respect to the control (ΔF_c), i.e. neurons only incubated with vehicle (DMSO at 0.1% in the Krebs-HEPES medium). Data are presented as percentage of blockade (100 - %ΔF) at the concentration of 10 μM, or as IC_{50}, i.e. the concentration of compound capable of halving the ΔF_c (%ΔF = 50)

4.19. Evaluation of the PP2A-performed phosphatase activity in SH-SY5Y cells

Cultures of SH-SY5Y neuroblastoma cells, according to protocol *4.17*, were preincubated with vehicle, test compounds or memantine at the desired concentration for 24 h. Then, medium was replaced by a fresh 1% FBS-supplemented MEM/F12 medium with the PP2A selective inhibitor OA at 15 nM, along with vehicle, test compounds or memantine at the desired concentration.

ACCEPTED MANUSCRIPT

Cells were challenged to the OA-evoked PP2A inhibition 18 h, after which the phosphatase activity was monitored by the method of the *p*NPP (cat. #786-453, VWR), according to the manufacturer guideline. The production of the chromogenic (λ_{max} = 405 nM) *para*-nitrophenolate from the *p*NPP dephosphorylation was allowed for 30 min at 37 ºC, and measured in a multi-well plate spectrophotometric reader (FluoStar Optima, BMG, Germany) at 405 nm.

4.20. Molecular modeling

Compound **12** was selected to predict the possible chemical interactions between PP2A and this family of **2** derivatives that could explain their pharmacological actions, as it was the best PAD according to the p*NPP* assays. Compound **12** was first modeled in Spartan 10 to obtain the most stable conformation in aqueous media, by molecular mechanic (*conformer distribution*), then refined by *ab initio* calculations with the 6-31G* base. After removing water and OA from the crystal complex, docking calculations for PP2A (PDB ID: 2IE4, www.rcsb.com) and **12** were inputted in Molegro Virtual Docker software, with enough binding sphere to cover the hole binding cavity, centered on the PP2Ac subunit, allowing ligand to freely pose. The pose with the lowest energy state, defined by the MolDock Score data (Table S1, supplementary material) was selected to characterize the chemical interactions with enzyme.

4.21. Viability experiments

ACCEPTED MANUSCRIPT

The effect of compounds **9–14** on the SH-SY5Y cells viability compromised by OA was evaluated by the method of the MTT reduction.[49] After 24 h of seeding, SH-SY5Y cells were preincubated with compounds at the concentration of 100 nM for 24 h. Afterwards, MEM/F12 medium was replaced by one fresh with 1% FBS, compounds at the same concentration, and OA, administered to media at the concentration of 20 nM. The viability of cultures were measured 20 h later, following a procedure recently described.[13]

4.22. Data Analysis

Sample sizes (*n*) for the experiments were calculated according to the formula $n = Z^2 \cdot s^2/e^2$, taking a confidence interval (*Z*) of 95%, error margin (*e*) of 5%, and a averaged standard deviation (*s*) of 0.05, obtaining a sample size of 3. The results represented in graphs are the means ± the standard error of the mean (S.E.M.). Comparison of data were considered statistically significant when *p* values were lower than 0.05, according to ANOVA statistical analyses followed by Newman-Keuls post hoc tests, calculated with GraphPad Prism 5.0 software under a Mac OS X-operated computer.

Acknowledgments

This work has been supported by grants from Instituto de Salud Carlos III (*Proyectos de Investigación en Salud*: PI13/00789 and PI16/00735, co-financed by FEDER) to CdlR. RLA and RLC thank Universidad Autónoma de Madrid for predoctoral fellowships. LV thanks Instituto de Salud Carlos III for predoctoral

ACCEPTED MANUSCRIPT

fellowship. We thank the continuous support of Instituto Fundación Teófilo Hernando.

Conflict of Interest

Authors declare no conflict of interests

A. Supplementary data

Supplementary data associated with this article can be found in the online version, at http://dx.doi.org/10.1016/j.bmc.2018.xx.xxx.

References and notes

1. Scheltens P, Blennow K, Breteler MM, de Strooper B, Frisoni GB, Salloway S, Van der Flier WM. Alzheimer's disease. *Lancet.* 2016.
2. Hardy JA, Higgins GA. Alzheimer's disease: the amyloid cascade hypothesis. *Science.* 1992;256:184–185.
3. Iqbal K, Liu F, Gong CX. Tau and neurodegenerative disease: the story so far. *Nat Rev Neurol.* 2016;12:15–27.
4. Davies P, Maloney AJ. Selective loss of central cholinergic neurons in Alzheimer's disease. *Lancet.* 1976;2:1403.
5. Selkoe DJ. Alzheimer's disease: a central role for amyloid. *J Neuropathol Exp Neurol.* 1994;53:438–447.

ACCEPTED MANUSCRIPT

6. Ehret MJ, Chamberlin KW. Current practices in the treatment of Alzheimer´s disease: where is the evidence after the phase III trials?. *Clin Ther.* 2015;37:1604–1616.

7. Alam S, Lingenfelter KS, Bender AM, Lindsley CW. Classics in chemical neuroscience: memantine. *ACS Chem Neurosci.* 2017;8:1823–1829.

8. Carreiras MC, Mendes E, Perry MJ, Francisco AP, Marco-Contelles J. The multifactorial nature of Alzheimer's disease for developing potential therapeutics. *Curr Top Med Chem.* 2013;13:1745–1770.

9. Prati F, Bottegoni G, Bolognesi ML, Cavalli A. BACE-1 inhibitors: from recent single-target molecules to multitarget compounds for Alzheimer's disease. *J Med Chem.* 2017;61:619–637.

10. Kosak U, Knez D, Coquelle N, Brus B, Pislar A, Nachon F, Brazzolotto X, Kos J, Colletier JP, Gobec S. N-Propargylpiperidines with naphthalene-2-carboxamide or naphthalene-2-sulfonamide moieties: potential multifunctional anti-Alzheimer's agents. *Bioorg Med Chem.* 2017;25:633–645.

11. Moreno-Ortega AJ, Martinez-Sanz FJ, Lajarin-Cuesta R, de Los Rios C, Cano-Abad MF. Benzothiazepine CGP37157 and its 2'-isopropyl analogue modulate Ca(2)(+) entry through CALHM1. *Neuropharmacol.* 2015;95:503–510.

12. Martinez-Sanz FJ, Lajarin-Cuesta R, Gonzalez-Lafuente L, Moreno-Ortega AJ, Punzon E, Cano-Abad MF, de Los Rios C. Neuroprotective profile of pyridothiazepines with blocking activity of the mitochondrial Na^{+}/Ca^{2+} exchanger. *Eur J Med Chem.* 2016;109:114–123.

13. Lajarín-Cuesta R, Nanclares C, Arranz-Tagarro JA, González-Lafuente L, Arribas RL, Araujo de Brito M, Gandía L, de los Ríos C. Gramine derivatives targeting Ca^{2+} channels and Ser/Thr phosphatases: a new dual strategy for the treatment of neurodegenerative diseases. *J Med Chem.* 2016;59:6265–6280.

14. Nimmrich V, Eckert A. Calcium channel blockers and dementia. *Br J Pharmacol.* 2013;169:1203–1210.

ACCEPTED MANUSCRIPT

15. Berridge MJ. Calcium hypothesis of Alzheimer's disease. *Pflügers Arch.* 2010;459:441–449.

16. Liu F, Grundke-Iqbal I, Iqbal K, Gong CX. Contributions of protein phosphatases PP1, PP2A, PP2B and PP5 to the regulation of tau phosphorylation. *Eur J Neurosci.* 2005;22:1942–1950.

17. Theendakara V, Bredesen DE, Rao RV. Downregulation of protein phosphatase 2A by Apolipoprotein E: Implications for Alzheimer's disease. *Mol Cell Neurosci.* 2017;83:83–91.

18. Arif M, Wei J, Zhang Q, Liu F, Basurto-Islas G, Grundke-Iqbal I, Iqbal K. Cytoplasmic retention of protein phosphatase 2A inhibitor 2 (I2PP2A) induces Alzheimer-like abnormal hyperphosphorylation of Tau. *J Biol Chem.* 2014;289:27677–27691.

19. Sontag E, Hladik C, Montgomery L, Luangpirom A, Mudrak I, Ogris E, White CL 3rd. Downregulation of protein phosphatase 2A carboxymethylation and methyltransferase may contribute to Alzheimer´s disease pathogenesis. *J Neuropathol Exp Neurol.* 2004;63:1080–1091.

20. Voronkov M, Braithwaite SP, Stock JB. Phosphoprotein phosphatase 2A: a novel druggable target for Alzheimer's disease. *Future Med Chem.* 2011;3:821–833.

21. Lajarin-Cuesta R, Arribas RL, De Los Rios C. Ligands for Ser/Thr phosphoprotein phosphatases: a patent review (2005–2015). *Expert Opin Ther Pat.* 2016;26:389–407.

22. Enjeti AK, D'Crus A, Melville K, Verrills NM, Rowlings P. A systematic evaluation of the safety and toxicity of fingolimod for its potential use in the treatment of acute myeloid leukaemia. *Anticancer Drugs.* 2016;27:560–568.

23. Malpas CB, Vivash L, Genc S, Saling MM, Desmond P, Steward C, Hicks RJ, Callahan J, Brodtmann A, Collins S, Macfarlane S, Corcoran NM, Hovens CM, Velakoulis D, O'Brien TJ. A phase IIa randomized control trial of VEL015 (sodium

ACCEPTED MANUSCRIPT

selenate) in mild-moderate Alzheimer's disease. *J Alzheimers Dis.* 2016;54:223–232.

24. Gonzalez-Lafuente L, Egea J, Leon R, Martinez-Sanz FJ, Monjas L, Perez C, Merino C, Garcia-De Diego AM, Rodriguez-Franco MI, Garcia AG, Villarroya M, Lopez MG, de Los Rios C. Benzothiazepine CGP37157 and its isosteric 2'-methyl analogue provide neuroprotection and block cell calcium entry. *ACS Chem Neurosci.* 2012;3:519–529.
25. Iwata S, Saito S, Kon-ya K, Shizuri Y, Ohizumi Y. Novel marine-derived halogen-containing gramine analogues induce vasorelaxation in isolated rat aorta. *Eur J Pharmacol.* 2001;432:63–70.
26. Hardingham GE, Bading H. Synaptic versus extrasynaptic NMDA receptor signalling: implications for neurodegenerative disorders. *Nat Rev Neurosci.* 2010;11:682–696.
27. Pumain R, Kurcewicz I, Louvel J. Ionic changes induced by excitatory amino acids in the rat cerebral cortex. *Can J Physiol Pharmacol.* 1987;65:1067–1077.
28. Reeve HL, Vaughan PF, Peers C. Calcium channel currents in undifferentiated human neuroblastoma SH-SY5Y cells: actions and possible interactions of dihydropyridines and omega-conotoxin. *Eur J Neurosci.* 1994;6:943–952.
29. Shuker MA, Bowser-Riley F, Davies SN. Possible NMDA antagonist properties of drugs that affect high pressure neurological syndrome. *Br J Pharmacol.* 1994;111:951–955.
30. Chan SF, Sucher NJ. An NMDA receptor signaling complex with protein phosphatase 2A. *J Neurosci.* 2001;21:7985–7992.
31. Kamat PK, Rai S, Nath C. Okadaic acid induced neurotoxicity: an emerging tool to study Alzheimer's disease pathology. *Neurotoxicology.* 2013;37:163–172.
32. Maidana M, Carlis V, Galhardi FG, Yunes JS, Geracitano LA, Monserrat JM, Barros DM. Effects of microcystins over short- and long-term memory and

ACCEPTED MANUSCRIPT

oxidative stress generation in hippocampus of rats. *Chem Biol Interact.* 2006;159:223–234.

33. Tian Q, Lin ZQ, Wang XC, Chen J, Wang Q, Gong CX, Wang JZ. Injection of okadaic acid into the meynert nucleus basalis of rat brain induces decreased acetylcholine level and spatial memory deficit. *Neuroscience.* 2004;126:277–284.

34. http://toxnet.nlm.nih.gov/cgi-bin/sis/search2/r?dbs+hsdb:@term+@DOCNO+7243, Hazardous Substance Data Bank (HSDB). Health & Human Services: Toxnet, Toxicology Data Network, 2005.

35. Schild A, Schmidt K, Lim YA, Ke Y, Ittner LM, Hemmings BA, Gotz J. Altered levels of PP2A regulatory B/PR55 isoforms indicate role in neuronal differentiation. *Int J Dev Neurosci.* 2006;24:437–443.

36. Chohan MO, Khatoon S, Iqbal IG, Iqbal K. Involvement of I2PP2A in the abnormal hyperphosphorylation of tau and its reversal by memantine. *FEBS Lett.* 2006;580:3973–3979.

37. Xing Y, Xu Y, Chen Y, Jeffrey PD, Chao Y, Lin Z, Li Z, Strack S, Stock JB, Shi Y. Structure of protein phosphatase 2A core enzyme bound to tumor-inducing toxins. *Cell.* 2006;127:341–353.

38. Takai A, Murata M, Torigoe K, Isobe M, Mieskes G, Yasumoto T. Inhibitory effect of okadaic acid derivatives on protein phosphatases. A study on structure-affinity relationship. *Biochem J.* 1992;284 (Pt 2):539–544.

39. Frydrychowski VA, Urbanek RA, Dounay AB, Forsyth CJ. Importance of the C28–C38 hydrophobic domain of okadaic acid for potent inhibition of protein serine-threonine phosphatases 1 and 2A. *Bioorg Med Chem Lett.* 2001;11:647–649.

40. Bohm HJ, Banner D, Bendels S, Kansy M, Kuhn B, Muller K, Obst-Sander U, Stahl M. Fluorine in medicinal chemistry. *Chembiochem.* 2004;5:637–643.

41. Costa AP, Tramontina AC, Biasibetti R, Batassini C, Lopes MW, Wartchow KM, Bernardi C, Tortorelli LS, Leal RB, Goncalves CA. Neuroglial alterations in rats

ACCEPTED MANUSCRIPT

submitted to the okadaic acid-induced model of dementia. *Behav Brain Res.* 2012;226:420–427.

42. Yi KD, Covey DF, Simpkins JW. Mechanism of okadaic acid-induced neuronal death and the effect of estrogens. *J Neurochem.* 2009;108:732–740.
43. Kamat PK, Rai S, Swarnkar S, Shukla R, Ali S, Najmi AK, Nath C. Okadaic acid-induced Tau phosphorylation in rat brain: role of NMDA receptor. *Neuroscience.* 2013;238:97–113.
44. Kamat PK, Tota S, Saxena G, Shukla R, Nath C. Okadaic acid (ICV) induced memory impairment in rats: a suitable experimental model to test anti-dementia activity. *Brain Res.* 2010;1309:66–74.
45. Kamat PK, Tota S, Shukla R, Ali S, Najmi AK, Nath C. Mitochondrial dysfunction: a crucial event in okadaic acid (ICV) induced memory impairment and apoptotic cell death in rat brain. *Pharmacol Biochem Behav.* 2011;100:311–319.
46. Valdiglesias V, Laffon B, Pasaro E, Cemeli E, Anderson D, Mendez J. Induction of oxidative DNA damage by the marine toxin okadaic acid depends on human cell type. *Toxicon.* 2011;57:882–888.
47. Ekinci FJ, Ortiz D, Shea TB. Okadaic acid mediates tau phosphorylation via sustained activation of the L-voltage-sensitive calcium channel. *Brain Res Mol Brain Res.* 2003;117:145–151.
48. Espadinha M, Dourado J, Lajarín-Cuesta R, Herrera-Arozamena C, Gonçalves LM, Rodríguez-Franco MI, de los Ríos C, Santos MM. Optimization of bicyclic lactam derivatives as NMDA receptor antagonists. *ChemMedChem.* 2017;12:537–545.
49. Denizot F, Lang R. Rapid colorimetric assay for cell growth and survival. Modifications to the tetrazolium dye procedure giving improved sensitivity and reliability. *J Immunol Methods.* 1986;89:271–277.

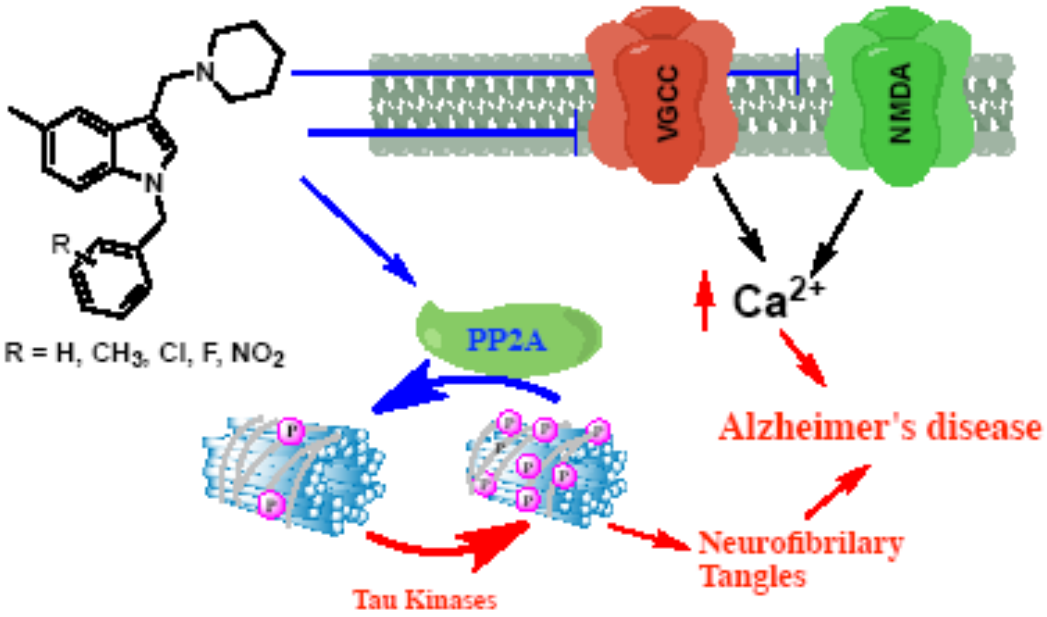

ACCEPTED MANUSCRIPT